

Exocomet signatures around the A-shell star ϕ Leo?

C. Eiroa¹, I. Rebollido¹, B. Montesinos², E. Villaver¹, O. Absil³, Th. Henning⁴, A. Bayo⁵, H. Canovas¹, A. Carmona⁶, Ch. Chen⁷, S. Ertel⁸, D. P. Iglesias⁵, R. Launhardt⁴, J. Maldonado⁹, G. Meeus¹, A. Moór¹⁰, A. Mora¹¹, A. J. Mustill¹², J. Olofsson⁵, P. Riviere-Marichalar¹³, and A. Roberge¹⁴

(Affiliations can be found after the references)

ABSTRACT

We present an intensive monitoring of high-resolution spectra of the Ca II K line in the A7IV shell star ϕ Leo at very short (minutes, hours), short (night to night), and medium (weeks, months) timescales. The spectra show remarkable variable absorptions on timescales of hours, days, and months. The characteristics of these sporadic events are very similar to most that are observed toward the debris disk host star β Pic, which are commonly interpreted as signs of the evaporation of solid, comet-like bodies grazing or falling onto the star. Therefore, our results suggest the presence of solid bodies around ϕ Leo. To our knowledge, with the exception of β Pic, our monitoring has the best time resolution at the mentioned timescales for a star with events attributed to exocomets. Assuming the cometary scenario and considering the timescales of our monitoring, our results indicate that ϕ Leo presents the richest environment with comet-like events known to date, second only to β Pic.

Key words. planetary systems – stars: individual: ϕ Leo – comets: general – circumstellar matter

1. Introduction

In spite of their low mass, Kuiper Belt objects, comets, and asteroids are key elements for understanding the early history of the solar system, its dynamics, and composition. While exoplanets are now routinely detected and hundreds of debris disks provide indirect evidence of planetesimals around main-sequence (MS) stars (Matthews et al. 2014), little is directly known about minor bodies around other stars than the Sun. The immense difficulty of a direct detection lies in their lack of a large surface area, which is required to detect their thermal or scattered emission. Dust features provide hints about the properties of μm -sized grains in debris disks that result from collisions of planetesimals (e.g. Olofsson et al. 2012). Circumstellar (CS) CO emission around some AF-type MS stars (e.g., Moór et al. 2015; Marino et al. 2016) has been interpreted to be the result of outgassing produced by comet collisions (Zuckerman & Song 2012). A complementary, somehow more direct, information on the exocomet nature and composition is provided by the detection of variable absorptions superposed on photospheric lines in the spectra of some stars.

Variable absorption features in metallic lines have been known for about 30 years in the optical spectrum of β Pic (Hobbs et al. 1985). These irregular features, mainly traced in the Ca II K line, appear redshifted and to a much lower degree blueshifted with respect to the radial velocity of the star, and might vary on timescales as short as hours. These features have been interpreted to be the result of the gas released by the evaporation of exocomets grazing or falling onto the star (Ferlet et al. 1987; Kiefer et al. 2014b, and references therein) that are driven into the vicinity of the star by the perturbing action of a larger body, that is, by a planet (Beust et al. 1991). Variable absorptions like this have also been observed toward several A-type stars (e.g., Redfield et al. 2007; Roberge & Weinberger 2008; Welsh & Montgomery 2015).

We have initiated a short- and medium-term high-resolution spectroscopic project aiming at detecting and monitoring these sporadic events that are attributed to exocomets in a sample of MS stars, most of them A-type stars, but also some FG-type stars with a range of ages. The sample includes stars for which exocomet signatures have been detected previously, such as 49 Ceti or HR 10, and also stars that have not been scrutinized yet for such events. So far, we have obtained more than 1200 spectra of about 100 stars (Rebollido et al., in preparation). The star ϕ Leo (HR 4368, HD 98058, HIP 55084) stands out as its spectrum exhibits conspicuous variations on timescales of hours, days, and months. This work presents our results concerning the Ca II K line obtained in five observing runs from December 2015 to May 2016. This line is particularly sensitive to these absorptions and is most frequently analyzed in the exocomet literature. Results for other relevant lines, including the Ca II IR-triplet, Ti II, Na I D, and Balmer lines, together with the spectra of other stars, will be presented in a forthcoming paper.

2. ϕ Leo: properties and astrophysical parameters

The source ϕ Leo is an A7IVn shell star (Jaschek et al. 1991) located at a distance of 56.5 pc. The star is seen close to edge-on with a very high rotational velocity, $v \sin i \sim 220 - 254$ km/s (Lagrange-Henri et al. 1990; Royer et al. 2007). It is surrounded by a gaseous CS disk detected in the Ti II 3685, 3759, 3762 Å lines and in the Ca II H/K lines (e.g., Jaschek et al. 1988; Abt 2008). The star ϕ Leo is close to the center of the local interstellar bubble, a cavity of low density, which makes it unlikely that its shell or disk is formed by accretion of the interstellar medium, as conjectured for other A-shell stars (Abt 2015). The Ca II K profile shows a triangular shape probably due to the combination of the photospheric and disk absorptions (Lagrange-Henri et al. 1990). The star does not possess a warm debris disk (Rieke et al. 2005), although a cool debris disk cannot be excluded since data

Table 1. Log of observations

Observing run	Dates	Spectra per night
2015 December ¹	20, 22, 23	1, 4, 1
2016 January ¹	27, 28, 30	1, 3, 3
2016 March ¹	3, 4, 5, 6	4, 4, 2, 3
2016 March ²	25, 26, 27, 28	4, 4, 3, 3
2016 May ¹	11	20

¹ HERMES, ² FEROS

at $\lambda > 25 \mu\text{m}$ do not exist, to our knowledge. The best Kurucz photospheric model fitting our spectra is $T_{\text{eff}} = 7500 \text{ K}$, $\log g = 3.75$, $v \sin i = 230 \text{ km/s}$, in good agreement with previous estimates (e.g., David & Hillenbrand 2015). Its bolometric luminosity is $\sim 45 L_{\odot}$ (Zorec & Royer 2012), and age estimates are in the range $\sim 500\text{-}900 \text{ Myr}$ (David & Hillenbrand 2015; De Rosa et al. 2014; Zorec & Royer 2012).

3. Observations

High-resolution spectra of ϕ Leo were obtained with the high-resolution fiber-fed échelle spectrographs HERMES and FEROS attached to the Mercator (La Palma, Spain) and MPG/ESO 2.2 m (La Silla, Chile) telescopes, respectively. A total of 60 spectra of ϕ Leo were taken. Observing dates, telescope, and number of spectra per night are given in Table 1. HERMES has a spectral resolution of ~ 85000 (high-resolution mode) covering the range $\lambda\lambda \sim 370\text{-}900 \text{ nm}$ (Raskin et al. 2011). Exposure times ranged from 260 to 600 seconds. Some spectra were taken consecutively and combined after reduction. FEROS has a spectral resolution $R \sim 48000$ covering the range from ~ 350 to 929 nm (Kaufer et al. 1999). Exposure times ranged from 120 to 360 seconds. The HERMES and FEROS spectra were reduced using the available pipelines of the two instruments. Barycentric corrections were also made for all spectra.

4. Results

Distinct changes are observed in the Ca II H and K lines of ϕ Leo. These changes affect the line profile as well as the wavelength and depth of the absorption peak. Variations occur on timescales of hours, days, and months. All the spectra show the triangular shape noted by Lagrange-Henri et al. (1990), modulated in most cases by additional redshifted absorption. Furthermore, we found no temporal variability pattern. In the following we refer to the Ca II K line alone, although we also comment on some Ca II H line spectra to illustrate the results for this line in comparison with the K line.

4.1. Stable Ca II K component

The Ca II K line spectra taken on 2015 December 20 and 23 are identical with their absorption peaks at the stellar radial velocity, $v_{\text{rad}} = -3 \text{ km/s}$ (de Bruijne & Eilers 2012). The remaining spectra are either deeper, with the absorption peak shifted to longer wavelengths, or with obvious additional redshifted absorption components superposed on the December 20 and 23 spectra. The exceptions are the spectra of 2016 March 3 and 5, which show small differences with those of December 20 and 23 (see below).

Figure 1 shows the average of the December 20 and 23 Ca II K line together with the photospheric line of the Kurucz model with stellar parameters mentioned in Sect. 2. The broad additional absorption with a FWHM = 56 km/s at approximately

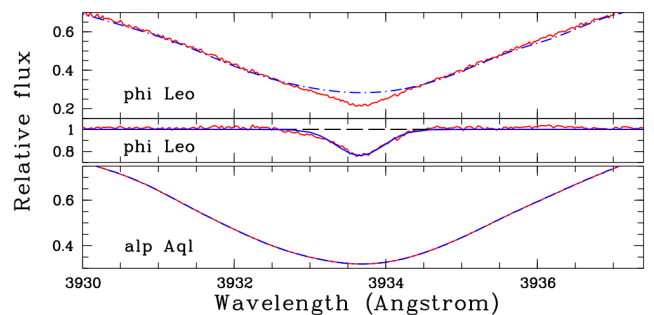


Fig. 1. Top: Average Ca II K line of ϕ Leo from 2015 December 20 and 23 (red continuous line), together with a Kurucz photospheric model (blue dash-dotted line). See text for stellar parameters. Middle: residuals of the average 20 and 23 spectra with respect to the photospheric line. The blue continuum line is a Gaussian with FWHM = 56 km/s. Bottom: observed Ca II K line (red line) of α Aql compared with a Kurucz model (blue dash-dotted line) with stellar parameters $T_{\text{eff}} = 7900 \text{ K}$, $\log g = 4.25$, $v \sin i = 210 \text{ km/s}$.

the stellar radial velocity produces the triangular shape of the line profile. Its depth and equivalent width are 0.238 and 0.22 Å, respectively. This corresponds to a column density $N(\text{Ca II}) \sim 2.3 \times 10^{12} \text{ cm}^{-2}$. To ensure that this additional absorption is real, we synthesized a photospheric model for α Aql, a star with similar spectral type (A7Vn) and rotational velocity, and compared it to spectra taken with the same instrument and configuration as for ϕ Leo. Figure 1 shows the excellent fit of the corresponding α Aql model to the observed spectra.

These results suggest that during December 20 and 23 we detected the contribution of a CS gas disk superposed on the stellar photosphere, while the remaining spectra are affected by additional gas absorptions, although other causes producing the triangular absorption cannot be excluded (see below). In the following we assume that the additional absorption seen on December 20 and 23 is a stable component in addition to the ϕ Leo photosphere and take the average of the two spectra as a template to analyze other contributions to the gas components.

4.2. Variable Ca II K components

Mercator 2015 December. The four spectra of December 22 show no appreciable changes, but their absorption is redshifted and deeper than the average December 20 and 23 template spectrum. Figure 2 shows the average of these four spectra and the residuals, taking the template spectrum as a continuum for the spectrum of December 22. An obvious absorption event occurs at $v \sim 6.0 \text{ km/s}$, that is, $\sim 9.0 \text{ km/s}$ redshifted from the stellar radial velocity, and depth ~ 0.083 . A second event might be present at a velocity $\sim 16 \text{ km/s}$ and depth ~ 0.060 . The equivalent width of both events together is $\sim 23 \text{ mÅ}$, and its FWHM is $\sim 25 \text{ km/s}$. The figure also shows the residuals corresponding to the Ca II H; in this case, only one event with a depth of ~ 0.054 is clearly seen.

Mercator 2016 January. These spectra appear slightly redshifted with respect to the template spectrum, but their depth is lower than the one of December 22. There might be tiny changes among the spectra taken on different nights, although we consider only their average because poor weather conditions produced relatively low signal-to-noise (S/N) ratios. Figure 2 shows the 2016 January spectrum and its residual compared to the template. An event at $\sim 15 \text{ km/s}$, that is, redshifted by $\sim 18 \text{ km/s}$ with respect to the stellar radial velocity, is clearly discernible. Its

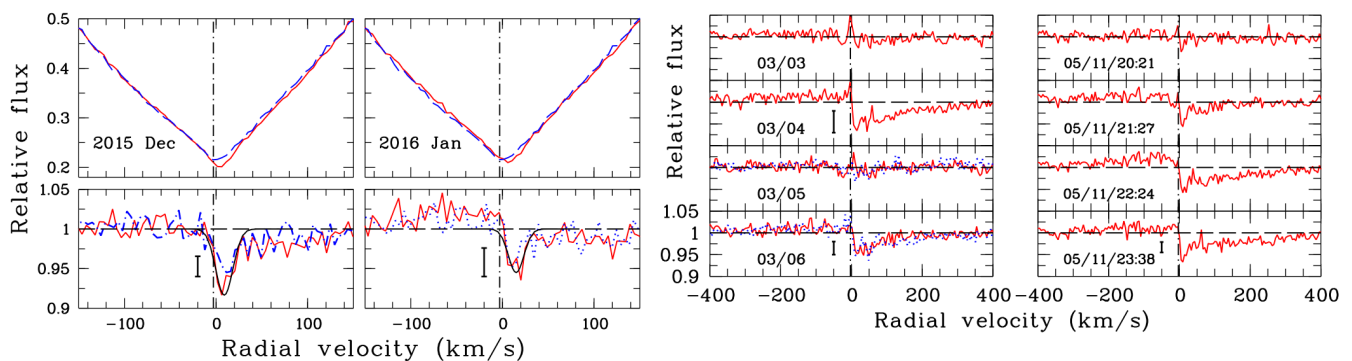


Fig. 2. From left to right the Ca II K line from the observing runs with Mercator. At the top of the December and January panels the average of the four December 22 spectra and the average of the January spectra are plotted (red continuous lines) together with the template spectrum (blue dashed line). At the bottom the corresponding residuals are shown in red. To guide the eye, two Gaussians with FWHM 25 km/s (December) and 20 km/s (January) are plotted (black continuous line). The March panel shows the residuals of the average spectrum of each night. The May panel shows the average of five consecutive spectra of May 11 starting at the UT indicated in the panel. Some panels show the residuals of the Ca II H line for comparison (blue dotted line). A $3\text{-}\sigma$ error bar is plotted in some panels. The dash-dotted line at -3.0 km/s corresponds to the radial velocity of the star.

equivalent width is $20 \text{ m}\text{\AA}$, the depth is 0.055, and the FWHM is ~ 20 km/s.

Mercator 2016 March. No detectable variations were recorded during the individual nights, but the Ca II K line clearly varied from night to night. Figure 2 shows the nightly residuals. The spectra of March 3 and 5 are similar to the template, but a clear flux depression is evident on March 4 and 6 at ~ 16 km/s, the March 4 depth of ~ 0.065 is deeper than the depth on March 6 of ~ 0.047 . In both cases, a broad wing extending up to ~ 200 km/s might be present. The corresponding Ca II H line depths are 0.052 and 0.047 for March 4 and 6, respectively.

Mercator 2016 May. Twenty spectra were taken consecutively during four hours on 2016 May 11. Figure 2 shows the Ca II K residuals with respect to the template spectrum grouped in four one-hour periods. The residuals smoothly change in one hour, and an event at ~ 9 km/s develops. Its deepest observed intensity of 0.068 depth is achieved during the last hour. A broad red wing seems to develop during the four observing hours.

MPG/ESO 2016 March. The Ca II K line exhibited a pronounced variation from night to night and within individual nights on timescales shorter than two hours. No regular pattern can be inferred from the variations. Figure 3 shows the average of the spectra taken during each of the four nights. All nights show a distinct redshifted event with respect to the template spectrum. Furthermore, the strength of the events changes strikingly from one spectrum to another, with time differences as short as 90 minutes. To exemplify this behavior, Fig. 3 shows the individual spectra from March 28 and March 29. Events at ~ 9 km/s and depths of 0.118 (March 28) and 0.093 (March 29) are detected. There might exist some blueshifted absorptions, at least on March 28, which vary in velocity, -4 to -9 km/s, and tiny changes in the depth of 0.04–0.05.

5. Discussion

The variable absorptions at 10–20 km/s from the star, with velocity dispersions of ~ 10 –20 km/s, depths of ~ 0.05 –0.1, and equivalent widths of $\sim 20 \text{ m}\text{\AA}$, that were observed in ϕ Leo behave similarly to those attributed to exocomets in β Pic. Nonetheless, it is reasonable to consider other alternatives because a remarkable difference between the two stars is that ϕ Leo is not associated with a massive debris disk. This might be due to the age of ϕ Leo because warm debris disks decline rapidly for stars older than a

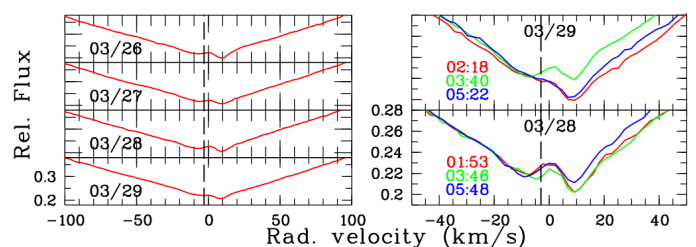


Fig. 3. Ca II K spectra obtained with the MPG/ESO 2.2 m telescope from March 26 to March 29. Right: average of the nightly spectra. Left: individual spectra taken during the nights March 28 and March 29. Colors correspond to the spectra obtained at different times (UT are shown).

characteristic time of ~ 150 Myr (Rieke et al. 2005). In addition, as noted before, it is unknown whether the star is surrounded by a cold debris disk, which in any case declines rapidly for stars older than a characteristic time of ~ 400 Myr (Su et al. 2006). Furthermore, some relatively old stars with exocomet signatures do not possess a debris disk (Roberge & Weinberger 2008).

For β Pic, phenomena involving the stellar atmosphere as the origin of the events were soon excluded (Lagrange-Henri et al. 1990). This seems also to be the case of ϕ Leo, since we would expect similar behavior in other photospheric lines, which is not the case. Moreover, given the very short timescales of the variations, an origin in the interstellar medium is not plausible. Mass-loss rates resulting from weak radiatively driven winds in A stars are not expected to be significant around late-type A7IV stars such as ϕ Leo. A wind origin like this was excluded for β Pic (Lagrange-Henri et al. 1992), although it has not been for events in other stars (Redfield et al. 2007). Sporadic mass-loss events, that is, clumps generated in a hypothetical stellar wind and rotating with the star, or moving outward with the wind, are expected to produce emission lines moving from blue to red across the center of the line, or be present in the blue and red wings of the wind lines. This is typically observed in relatively hot stars, like Be stars (Porter & Rivinius 2003). However, this behavior is not observed in ϕ Leo.

The ratio of the event depths observed in the Ca II K and H lines, ~ 1 –1.5, differs from the oscillator strength ratio of these lines ($=2$), suggesting that the variable absorptions arise at least partly from optically thick clumpy gas that covers a small fraction of the stellar surface, again similar to β Pic or HD 172555

(Lecavelier Des Etangs et al. 1997; Kiefer et al. 2014a). These results, together with the high-velocity broad line wings suggested in some spectra, makes it plausible that the ϕ Leo events trace the evaporation of comet-like bodies in the CS environment. In this scenario, the broad wings could be produced by a sort of comet-like coma or by several unresolved events.

Assuming a cometary origin, the similar dynamical properties of the events could point to a disruption of a larger primordial body by tidal forces in a near-stellar encounter, or to a family of comets (Beust et al. 1996) driven into the vicinity of the star by a planet. Several not mutually exclusive mechanisms might deliver the bodies: Kozai-Lidov (Naoz 2016), secular resonances (Levison et al. 1994), mean motion resonances (Beust & Morbidelli 1996), or direct scattering by an eccentric planet (Beust et al. 1991). We note that only a future improvement of the event statistics in ϕ Leo will help to better constrain these dynamical mechanisms. The orbit of the infalling bodies can only be roughly estimated since the radial velocity is degenerated between the pericenter distance and the angle formed between the axis of the orbit and the line of sight (true anomaly). Thus, the largest pericenter distances at which the bodies can originate (for a $3.25 M_{\odot}$ star, estimated from the stellar parameters in Sect. 2) is ~ 20 -70 au. The observed infall velocities, ~ 0 -20 km/s, possibly with some wings of up to 200 km/s, are much lower than the free-fall velocity at reasonable pericenter distances, 79 km/s and 177 km/s at 50 and 10 R_{\star} , respectively. The most plausible option apparently is that the presumable exocomets follow parabolic to hyperbolic orbits that cross the line of sight, in which case the main absorption event and the broad wings at larger velocities can be explained. The crossing distances must be close enough to the star to allow refractory material to sublimate. Following Beust et al. (1998), the shortest crossing distance would be ~ 0.21 au using a FWHM of 20 km/s and assuming that the source of broadening the line is Keplerian. Alternatively, if we assume thermal equilibrium (Beust et al. 1996), the distance at which dust sublimates, taking as a typical value $T_{\text{sub}} = 1500$ K, would be ~ 0.46 au or ~ 0.33 au for albedos 0.0 and 0.5, respectively. These values depend on the composition of the grains.

With respect to the stable Ca II component, we can exclude it originates in the local interstellar medium since interstellar lines are considerably narrower, the line of sight traverses the Leo cloud, which has a centroid radial velocity of 1.75 km/s (Redfield & Linsky 2008), and its equivalent width gives a lower limit for the column density of $N(H) \gtrsim 10^{20} \text{cm}^{-2}$, much higher than the expected interstellar column densities in the Leo direction (Redfield & Linsky 2000). This means that the component might originate in one of the scenarios suggested for the stable CS gas disk in β Pic: stellar winds, star-grazing comet evaporation, or grain evaporation near the star or in the disk (see Fernández et al. 2006), although we note that the stable ϕ Leo component is broader and not as sharp as in β Pic (Lagrange-Henri et al. 1992). On the other hand, practically all stars showing a triangular shape rotate at very high velocities, $v \sin i \gtrsim 200$ km/s. At these velocities the structure of the rotating stars and the inclination angle with respect to the line of sight affect their location on color-magnitude diagrams (Bastian & de Mink 2009), and the induced oblateness of the star produces a gravity darkening that results from the temperature gradient from the stellar equator to the poles. A preliminary test for which Kurucz models were combined with a temperature gradient from the equator to the poles indicated that the strength of the additional triangular absorption decreases. A deeper analysis has been undertaken (Montesinos et al., in preparation).

6. Conclusions

Our intensive monitoring of ϕ Leo showed that its spectrum is very rich in redshifted absorption events, which might be accompanied in some cases by broad wings and even blueshifted absorptions. These sporadic events are similar to those in β Pic and can be most plausibly explained as exocomets that graze the star or fall onto the stellar surface. Assuming this scenario, it is intriguing how a relatively old 500-900 Myr star such as ϕ Leo, which does not have any known associated debris disk, can possess such a rich environment that hosts minor bodies. Another interesting aspect is the origin of what might be a triangular-shaped stable CS absorption component in the Ca II lines. Additional monitoring is clearly needed to better characterize the sporadic events and the stable component by comparing them with similar stars.

Acknowledgements. Based on observations made with the Mercator Telescope, operated on the island of La Palma by the Flemish Community, at the Spanish Observatorio del Roque de los Muchachos of the Instituto de Astrofísica de Canarias. H.C., C.E., G. M., B. M., I. R., and E.V. are supported by Spanish grant AYA 2014-55840-P. J.O. acknowledges support from ALMA/Conicyt Project 31130027. O.A. is F.R.S.-FNRS Research Associate. We thank the referee H. Beust for his constructive comments.

References

- Abt, H. A. 2008, *ApJS*, 174, 499
 Abt, H. A. 2015, *PASP*, 127, 1218
 Bastian, N. & de Mink, S. E. 2009, *MNRAS*, 398, L11
 Beust, H., Lagrange, A.-M., Crawford, I. A., et al. 1998, *A&A*, 338, 1015
 Beust, H., Lagrange, A.-M., Plazy, F., & Mouillet, D. 1996, *A&A*, 310, 181
 Beust, H. & Morbidelli, A. 1996, *Icarus*, 120, 358
 Beust, H., Vidal-Madjar, A., & Ferlet, R. 1991, *A&A*, 247, 505
 David, T. J. & Hillenbrand, L. A. 2015, *ApJ*, 804, 146
 de Bruijne, J. H. J. & Eilers, A.-C. 2012, *A&A*, 546, A61
 De Rosa, R. J., Patience, J., Wilson, P. A., et al. 2014, *MNRAS*, 437, 1216
 Ferlet, R., Vidal-Madjar, A., & Hobbs, L. M. 1987, *A&A*, 185, 267
 Fernández, R., Brandeker, A., & Wu, Y. 2006, *ApJ*, 643, 509
 Hobbs, L. M., Vidal-Madjar, A., Ferlet, R., Albert, C. E., & Gry, C. 1985, *ApJ*, 293, L29
 Jасhek, M., Jасhek, C., & Andriillat, Y. 1988, *A&AS*, 72, 505
 Jасhek, M., Jасhek, C., & Andriillat, Y. 1991, *A&A*, 250, 127
 Kaufer, A., Stahl, O., Tubbesing, S., et al. 1999, *The Messenger*, 95, 8
 Kiefer, F., Lecavelier des Etangs, A., Augereau, J.-C., et al. 2014a, *A&A*, 561, L10
 Kiefer, F., Lecavelier des Etangs, A., Boissier, J., et al. 2014b, *Nature*, 514, 462
 Lagrange-Henri, A. M., Ferlet, R., Vidal-Madjar, A., et al. 1990, *A&AS*, 85, 1089
 Lagrange-Henri, A. M., Gosset, E., Beust, H., Ferlet, R., & Vidal-Madjar, A. 1992, *A&A*, 264, 637
 Lecavelier Des Etangs, A., Deleuil, M., Vidal-Madjar, A., et al. 1997, *A&A*, 325, 228
 Levison, H. F., Duncan, M. J., & Wetherill, G. W. 1994, *Nature*, 372, 441
 Marino, S., Matrà, L., Stark, C., et al. 2016, *MNRAS*, 460, 2933
 Matthews, B. C., Krivov, A. V., Wyatt, M. C., Bryden, G., & Eiroa, C. 2014, *Protostars and Planets VI*, 521
 Moór, A., Henning, T., Juhász, A., et al. 2015, *ApJ*, 814, 42
 Naoz, S. 2016, *ArXiv e-prints [arXiv:1601.07175]*
 Olofsson, J., Juhász, A., Henning, T., et al. 2012, *A&A*, 542, A90
 Porter, J. M. & Rivinius, T. 2003, *PASP*, 115, 1153
 Raskin, G., van Winckel, H., Hensberge, H., et al. 2011, *A&A*, 526, A69
 Redfield, S., Kessler-Silacci, J. E., & Cieza, L. A. 2007, *ApJ*, 661, 944
 Redfield, S. & Linsky, J. L. 2000, *ApJ*, 534, 825
 Redfield, S. & Linsky, J. L. 2008, *ApJ*, 673, 283
 Rieke, G. H., Su, K. Y. L., Stansberry, J. A., et al. 2005, *ApJ*, 620, 1010
 Roberge, A. & Weinberger, A. J. 2008, *ApJ*, 676, 509
 Royer, F., Zorec, J., & Gómez, A. E. 2007, *A&A*, 463, 671
 Su, K. Y. L., Rieke, G. H., Stansberry, J. A., et al. 2006, *ApJ*, 653, 675
 Welsh, B. Y. & Montgomery, S. L. 2015, *Advances in Astronomy*, 2015, 980323
 Zorec, J. & Royer, F. 2012, *A&A*, 537, A120
 Zuckerman, B. & Song, I. 2012, *ApJ*, 758, 77

-
- ¹ Dpto. Física Teórica, Universidad Autónoma de Madrid, Cantoblanco, 28049 Madrid, Spain, e-mail: carlos.eiroa@uam.es
 - ² CAB (CSIC-INTA), Camino Bajo del Castillo, s/n, 28692 Villanueva de la Cañada, Madrid, Spain
 - ³ STAR Institute, Université de Liège, F.R.S.-FNRS, 19c Allée du Six Août, B-4000 Liège, Belgium
 - ⁴ Max-Planck-Institut für Astronomie (MPIA), Königstuhl 17, D-69117 Heidelberg, Germany
 - ⁵ Instituto de Física y Astronomía, Facultad de Ciencias, Universidad de Valparaíso, 5030 Casilla, Valparaíso, Chile
 - ⁶ Université de Toulouse, UPS-OMP, IRAP, Toulouse F-31400, France
 - ⁷ Space Telescope Science Institute, 3700 San Martin Drive, Baltimore, MD 21212, USA
 - ⁸ Steward Observatory, Department of Astronomy, University of Arizona, Tucson, AZ 85721, USA
 - ⁹ INAF, Osservatorio Astronomico di Palermo, 90134 Palermo, Italy
 - ¹⁰ Konkoly Observatory, Research Centre for Astronomy and Earth Sciences, PO Box 67, 1525 Budapest, Hungary
 - ¹¹ Aurora Technology B.V. for ESA, ESA-ESAC, Camino Bajo del Castillo, s/n, 28692 Villanueva de la Cañada, Madrid, Spain
 - ¹² Lund Observatory, Department of Astronomy and Theoretical Physics, Lund University, Box 43, SE-221 00 Lund, Sweden
 - ¹³ ESA-ESAC, Camino Bajo del Castillo, s/n, 28692 Villanueva de la Cañada, Madrid, Spain
 - ¹⁴ Exoplanets & Stellar Astrophysics Lab, NASA Goddard Space Flight Center, Code 667, Greenbelt, MD 20771, USA